INTRODUCTION

This report describes research activities that were performed during the third phase of a program designed to investigate the mechanism of strengthening and fracture in composite materials. As mentioned in previous reports, three different types of composite are currently being investigated. These are discussed separately in the following paragraphs:

I. The Mechanisms of Strengthening and Fracture in Composites Containing Hard Particles Dispersed in a Softer Matrix

a) Tensile and Impact Deformation of Hypo-Eutectoid Steels
(with Darel Hodgson, Graduate Student)

Hypo-eutectoid steels are of interest because the ferrite matrix, and hence the composite as a whole, can be made to undergo a ductile-brittle transition by changing the test temperature and the morphology of the hard carbide (Fe_3C) particles by heat treatment.

To study the effect of varying carbide morphology, two steels containing 0.4 and 0.6% carbon were tested in uniaxial tension under plane stress conditions in both the pearlitic and spheroidized forms. The tests were conducted at temperatures from room temperature to - 196°C to determine the effect of carbide morphology on the ductile to brittle transition.

In the pearlitic steels, composed of lamellar pearlite and pro-eutectoid ferrite, a ductile-brittle transition was observed at about - 150°C for both the 0.4 and 0.6 percent carbon steels. The similarity of this transition to published results for a low carbon (0.2%)steel of the same ferrite grain size leads to the conclusion* that the transition

* Hodgson, Darel, M. S. Thesis, Stanford University, September, 1965)

temperature is determined solely by the properties of the pro-eutectoid ferrite. Increasing the carbon content (i.e., the amount of lamellar pearlite) serves only to refine the pro-eutectoid ferrite grains and constrain yielding in the ferrite. While both of these effects raise the tensile yield stress, σ_Y, the cleavage fracture stress σ_f is also raised by the grain size refinement. Consequently, the ductility transition temperature (i.e., the highest temperature at which $\sigma_Y = \sigma_f$) is essentially unchanged by increasing pearlite additions.

The spheroidized steels were quite ductile at all temperatures down to - 196°C. They had a fine ferrite grain size (ASTM No. 13) and a homogeneous distribution of spheroidal carbides of about 0.5 micron average diameter. The high ductility of the spheroidized steels may be ascribed to the extremely fine carbide particles and fine ferrite grain size. The latter prevented the nucleation of microcracks in the ferrite. It was observed that a number of the larger carbide particles near the fracture surface were cracked in all of the specimens. In some cases, these cracks had begun to open up and form voids.

Brittle fracture in medium and high strength steels occurs by the formation of voids (at cracked carbides or inclusions) and the coalescence of these voids by internal necking on a microscopic scale. It is known that the fracture toughness K_{Ic} decreases with increasing strength level (σ_Y) and increasing volume fraction of large particles (e.g., inclusions) but the relation between these two variables has never been investigated in detail. Quenched and tempered hypo-eutectoid steels serve as excellent model materials on which to perform this investigation since their yield strength level can be varied (for a constant particle size) by

varying the test temperature while the particle (i.e., carbide) size can be varied by heat treatment.

Six vacuum melted and rolled hypo-eutectoid steels containing various carbon and manganese contents have been studied to determine the optimum heat treatment for obtaining spheroidized carbides of various sizes. It was determined that austenizing for one hour at 1100°C followed by oil quenching from 825°C and tempering at 700°C for times up to 24 hours yields a homogeneous, spheroidized microstructure containing carbide particles whose diameter varies up to 10 microns. All heat treatments were conducted in static vacuum and no observable decarburization was found.

Slow bend specimens have been machined from three of the steels and a number of these specimens have been heat treated as described above. A slow bend jig and temperature controlling device has been constructed and bend testing has begun on one of the steels. Once the fracture load and general yield load has been determined as a function of test temperature, specimens will be loaded to various fractions of the fracture load, unloaded, sectioned, and examined by optical and replica electron microscopy. The number of cracked particles near the notch root will be determined, and the process of void coalescence during slow crack growth will be observed, as a function of nominal stress, yield strength level, and carbide size.

b) Tensile Micro-Strain Studies of TiC-Ni-Mo Cermets
(with F. Darwish, Graduate Student)

The purpose of this investigation is to determine the mechanism of fracture in a composite containing large volume fractions of TiC dispersed in a soft matrix of Ni and Mo. Mo additions to Ni enhance the

wetting of the TiC particles by the liquid phase during final sintering and this results in a refinement of the carbide grain size.

During the last period the following progress has been made. Composite powders with different particle size, as described in PR2, have been prepared. Green compacts have been produced by pressing the composite powder at a pressure of 20,000 p.s.i. in a dog-bone-shaped die. The compacts are currently being pre-sintered in a hydrogen atmosphere at 1200°F; the binder being burned off by heating at 400°F for one hour.

The high frequency induction generator has arrived, power has been connected, and a new water pipeline is being extended to the generator. The Mo conductor and the heat shields have been completed. A thermocouple, saturable core reactor control and a controller calibrated for the thermocouple will be used to control the final sintering temperature. The pre-sintered compacts will be final sintered at 2500°F for a period of one hour independent of their composition. The final sintered compacts will be ground, and tested on the microstrain apparatus. The density of microcracks in the TiC particles will be determined as function of the microstrain using replication techniques and optical and electron microscopy.

II. Theoretical Aspects of Fracture in Composite Materials
(with D. Barnett, Graduate Student)

Dislocation interactions with elastic inhomogeneities of various shapes are currently being studied. The investigation should yield information of practical importance in fiber or laminate strengthened composite materials which contain large inclusions (inclusions whose mean diameter is $\geq$ 1000 Å) and are therefore subject to ductile fracture by

void formation around the inclusions and subsequent void growth and coalescence.

The problem of void formation about inclusions is being approached in the following manner. Because the inclusions are quite rigid relative to the ductile matrix containing them, plastic flow in the matrix may result in dislocation pileups at the particle-matrix interface. The resulting stress concentration may lead to particle fracture or interface cracking, depending upon the relative magnitude of surface energies involved as well as upon particle shape, size, and curvature.

The stress concentration due to pileups at various shaped inclusions is best treated by the method of continuously distributed dislocations. Two of the problems being investigated are screw and edge dislocation pileups at cylindrical inclusions and at laminates or fibers. The screw pileup at a cylindrical inclusion generates the following singular integral equation for the dislocation distribution function f(t):

$$\int_a^{a+L} \frac{f(t)dt}{x-t} + \int_a^{a+L} \frac{f(t)dt}{x - \frac{a^2}{t}} - \frac{N}{x} = \frac{2\pi\tau}{\mu_1 b}$$

There are N dislocations in the slip line of length L, τ is the applied shear stress, "a" is the particle radius, μ_1 the matrix shear modulus, and x is the distance from the center of the particle to a point on the slip plane (Figure 1a). This equation may also be written

$$\int_a^{a+L} \frac{f(t)dt}{x' - t} + \int_a^{a+L} \frac{f(t)dt}{x' - \frac{a^2}{t}} - \frac{N}{x'} = \frac{2\pi\tau}{\mu_1 b} \quad \text{for } x' > a$$

By defining new variables $x = ax'$, $t' = at$, and by noting that from the

asymmetry of the pileup and its image that $f\left(\frac{1}{t}\right) = t^2 f(t)$, the equation may be recast as

$$\int_{1/\beta}^{\beta} \frac{f(t)dt}{x-t} = -\frac{N}{x} + \frac{2\pi a\tau}{\mu_1 b} \quad \text{for } x>1;\ \beta = 1 + \frac{L}{a}$$

$$= -\frac{N}{x} - \frac{2\pi a\tau}{\mu_1 b x^2} \quad \text{for } x<1$$

The solution is

$$f(x) = \frac{2a\tau}{\pi\mu_1 b}\left[\left(\frac{\pi}{2} + \sin^{-1}\frac{\beta-1}{\beta+1}\right)\left(\frac{1}{x} + \frac{1}{x^2}\right)\sqrt{(\beta-x)(x-1/\beta)}\right.$$

$$\left. + \left(1 + \frac{1}{x^2}\right)\left\{\ell n \frac{\beta-1}{\beta+1}\frac{x+1}{|x-1|}\left[1 + 2\frac{\sqrt{\beta-x}\sqrt{\beta x-1}}{(\beta-1)(x+1)}\right]\right\}\right]$$

Note: $f(x) = \frac{1}{x^2} f\left(\frac{1}{x}\right)$

with the condition

$$\frac{\mu_1 Nb}{2\tau L} = \frac{1}{\sqrt{\beta}} + \frac{\beta-1}{2\beta}\left\{\frac{\pi}{2} + \sin^{-1}\frac{\beta-1}{\beta+1}\right\}$$

The last condition gives N as a function of a and L and yields the correct answer for:

(1) $a \to \infty$ (Chou's soln. for semi-infinite second phase)

(2) $a \to o$ (Stroh's soln. for homogeneous material)

Knowing f(t), the stresses in the particle and at the interface can be calculated and this will be done shortly. The equation for the edge pileup is considerably more complex due to additional terms involving image dislocation multipoles, but presumably the solution for the screw pileup will yield insight for treating the edge problem.

The laminate or fiber problem has been formulated and it does not appear that the distribution function f(t) is much different from that of a semi-infinite second phase as treated by Chou. Chou's results have

been extended by actually calculating the stresses present in the second phase and at the interface in closed form. All stresses have the form (in polar co-ordinates)

$\sigma_{ij} = F_{ij}(\theta)\ \ell n\ (2L/r)$, where r is the distance from the pileup tip for the case of an edge dislocation pileup. The values of F_{ij} are shown in Figure 1b.

The problem of interface cracking is being treated by classical elasticity methods. For the two above cases this means obtaining solutions for

(1) The T - Crack

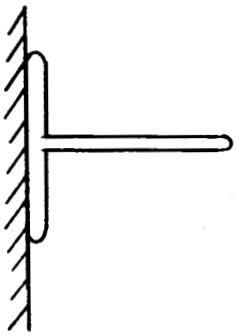

(2) The Circular Arc Crack

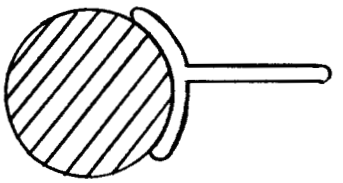

Criteria for void formation and crack blunting in composites can then be formulated and applied to McClintock's earlier work on fracture by void coalescence.

III. <u>The Mechanism of Fracture in Composites of Mechanically Drilled Holes and a B.C.C. Metal Matrix</u>

(with Charles A. Rau, Jr., Graduate Student)

Small drilled holes can markedly improve the toughness of specimens containing sharp notches. It was previously reported (PR 2) that two holes drilled in the yield zones of a notched sample lowered the charpy impact transition temperature of iron - 2% nickel alloy by as

much as 35°C depending on their position. During the past six months, we have:

(1) Performed additional charpy impact tests and

(a) Further defined the important geometrical parameters locating the holes.

(b) Shown that similar increases in notch-toughness can be achieved by holes which are drilled only partially through the specimen thickness.

(c) Shown that the impact energy required to produce low energy tear fracture in charpy samples of ultra-high strength steel (250 grade Maraging) is doubled when appropriately drilled holes are present.

(2) Performed slow-bend tests on charpy-type samples and

(a) Shown that the load carrying capacity of notched samples can be increased significantly (up to 70% greater in Fe - 2% Ni) at low temperatures where samples cleave prior to general yielding.

(b) Shown that drilled samples have a lower general yield load than standard notched samples and require much larger bend angles to produce fracture after general yield at a given temperature.

(3) Observed the redistribution of strain around a notch caused by drilled holes by dislocation etch-pitting of Fe-3% Si notch-bend samples which had been loaded to various fractions of their general yield load.

The charpy (1), slow bend (2), and portions of the etch-pitting (3) results have been reported in detail*. Metallographic examination of the

* Tetelman, A.S. and Rau, C.A., Jr., Technical Report #1 (NASA-NSG-622) August, 1965

surface of etch-pitted specimens revealed that the holes cause a pronounced redistribution of strain around the notch (see Tech. Rept. #1).

Subsequent etch-pitting studies have revealed the variation in the strain patterns from the specimen surface (plane stress) to its center (plane strain). Figures 2a and 2b show the effect of the holes on the strain distribution midway between the surface and the center of specimens loaded to 50% of general yield. Similar patterns were observed in the specimen center demonstrating that in the critical plane strain regions the holes redistribute the plastic away from the notch tip. Thus the plastic stress concentration factor is lower than for the undrilled sample at any given bend angle. Attainment of the cleavage stress below the notch tip requires much larger displacements (bend angles) while fracture is encouraged to initiate between the notch sides and each hole by the high strains present there. Once fracture occurs to both holes the mechanism described in Technical Report #1 operates producing the observed improvements in notch toughness.

Preliminary results have indicated that the magnitude of the improvement with holes is a function of the ease of fibrous or shear failure in the material itself. Future work will employ a series of different hypo-eutectoid steels to study this effect in more detail. Notched sheet tensile specimens of Fe-3% Si alloy will be used to (1) define the nature of the reduction in plastic constraint produced by the holes, and (2) determine the changes in optimum geometrical parameters resulting from tensile loading and plane stress conditions. A determination of the effect of more complex arrays of holes on notch toughness in tension and bending shall also be made.

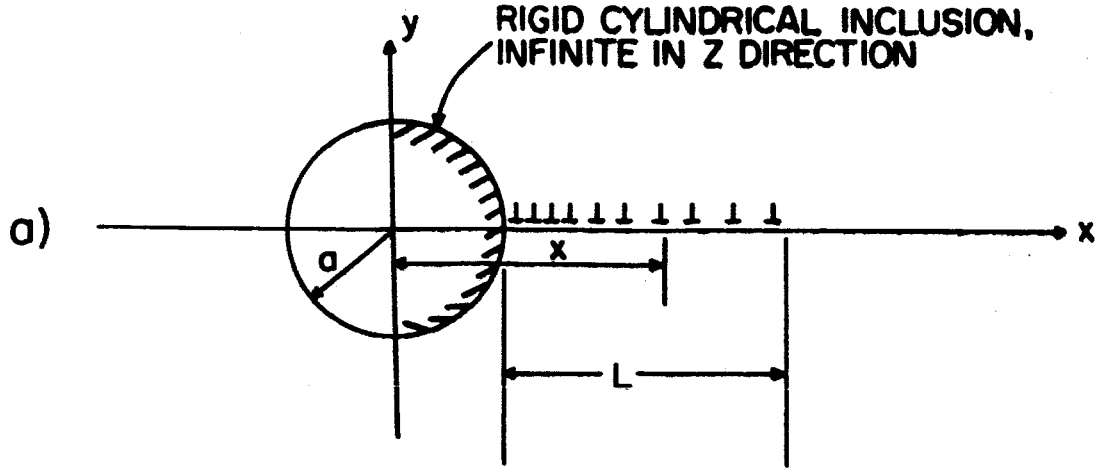

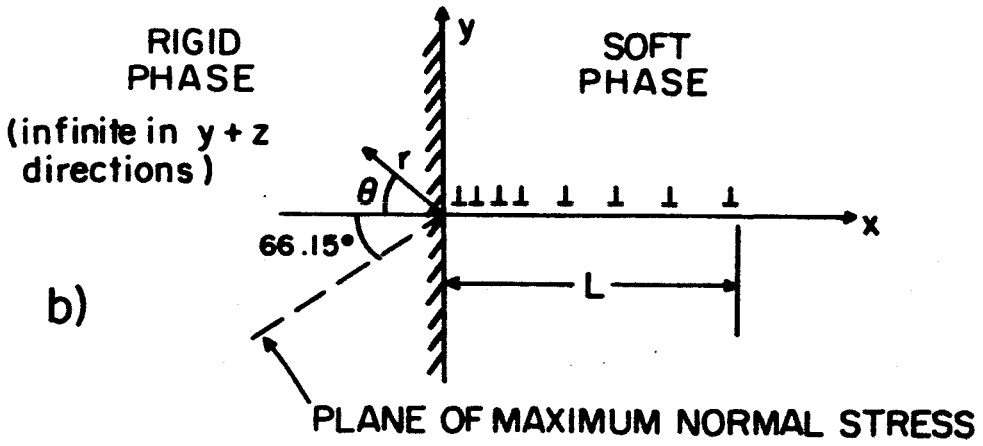

FOR $L \gg r$

$$\tau_{xx} = -\frac{8\tau}{\pi^2}\left\{\theta + 1/2 \sin 2\theta\right\} \ln \frac{2L}{r}$$

$$\tau_{yy} = -\frac{8\tau}{\pi^2}\left\{\theta + 1/2 \sin 2\theta\right\} \ln \frac{2L}{r}$$

$$\tau_{xy} = \frac{8\tau}{\pi^2} \cos^2\theta \ln \frac{2L}{r}$$

$$\tau_{xx})_{\text{INTERFACE}} = \frac{4\tau}{\pi} \ln \frac{2L}{|y|}$$

MAXIMUM NORMAL STRESS IN SECOND PHASE OCCURS ALONG A PLANE AT $\theta = 66.15°$

Figure 1

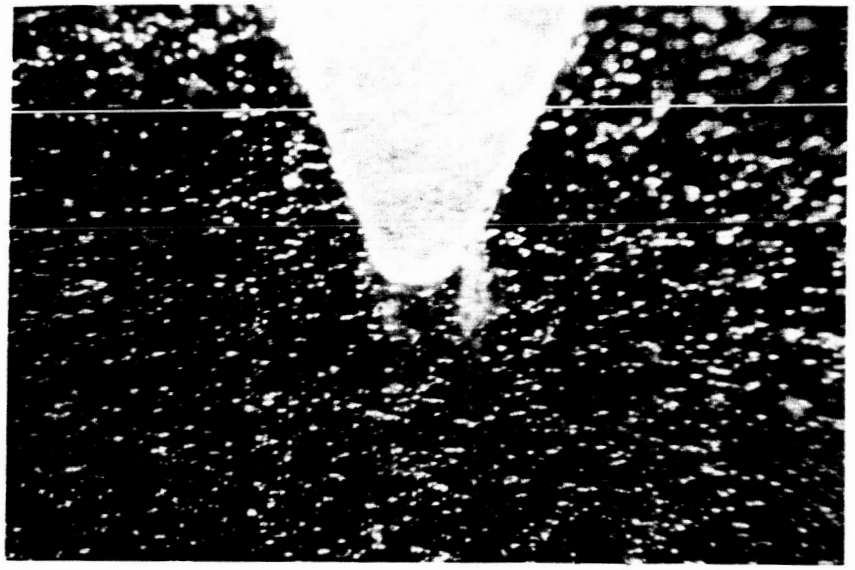

(a)

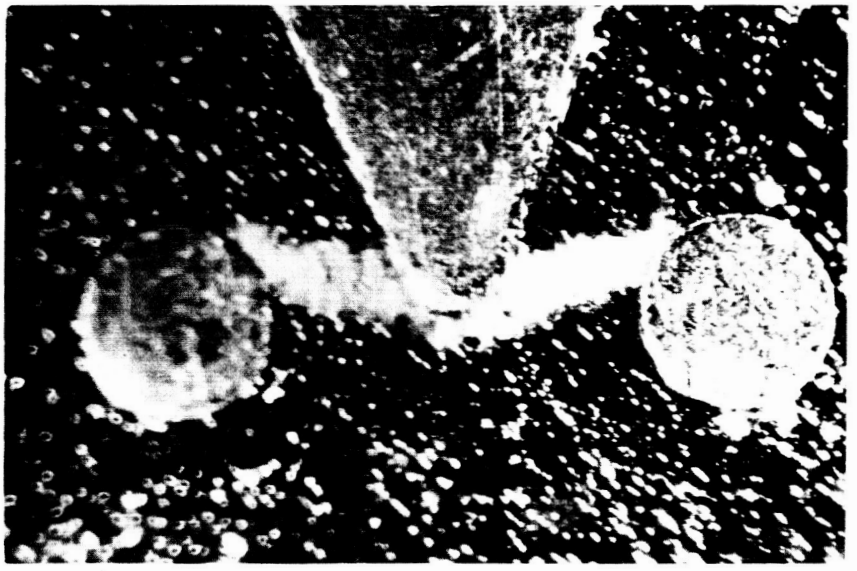

Figure 2. Comparison of the yielded zones of a Standard (a) and drilled (b) Fe-3% Si specimen midway between the specimen surface and midsection after loading to 50% of their respective general yield loads in pure bending. Mignification: 30X